Endocrinology. 2013. 154(3): 1321-1336

Distinct expression patterns predict differential roles of the miRNA-binding proteins, Lin28 and Lin28b, in the mouse testis: studies during postnatal development and in a model of hypogonadotropic hypogonadism

Francisco Gaytan, Susana Sangiao-Alvarellos, María Manfredi-Lozano, David García-Galiano, Francisco Ruiz-Pino, Antonio Romero-Ruiz, Silvia León, Concepción Morales, Fernando Cordido, Leonor Pinilla, and Manuel Tena-Sempere

Abstract

Lin28 (also termed Lin28a) and Lin28b are related RNA-binding proteins, involved in the control of microRNA synthesis, especially of the let-7 family, with putative functions in early (embryo) development. However, their roles during postnatal maturation remain ill defined. Despite the general assumption that Lin28 and Lin28b share similar targets and functions, conclusive demonstration of such redundancy is still missing. In addition, recent observations suggest a role of Lin28 proteins in mammalian reproduction, which is yet to be defined. We document herein the patterns of RNA expression and protein distribution of Lin28 and Lin28b in mouse testis during postnatal development and in a model of hypogonadotropic hypogonadism as a result of inactivation of the kisspeptin receptor, Gpr54. Lin28 and Lin28b mRNAs were expressed in mouse testis across postnatal maturation, but their levels disparately varied between neonatal and pubertal periods, with peak Lin28 levels in infantile testes and sustained elevation of Lin28b mRNA in young adult male gonads, where relative levels of let-7a and let-7b miRNAs were significantly suppressed. In addition, Lin28 peptides displayed totally different patterns of cellular distribution in mouse testis: Lin28 was located in undifferentiated and type-A1 spermatogonia, whereas Lin28b was confined to spermatids and interstitial Leydig cells. These profiles were perturbed in Gpr54 null mouse testis, which showed preserved but irregular Lin28 signal and absence of Lin28b peptide, which was rescued by administration of gonadotropins, mainly hCG (as super-agonist of LH). In addition, increased relative levels of Lin28, but not Lin28b, mRNA and of let-7a/let-7b miRNAs were observed in Gpr54 KO mouse testes. Altogether, our data are the first to document the divergent patterns of cellular distribution and mRNA expression of Lin28 and Lin28b in the mouse testis along postnatal maturation and their alteration in a model of congenital hypogonadotropic hypogonadism. Our findings suggest distinct functional roles of these two related, but not overlapping, miRNA-binding proteins in the male gonad.

Lin28 was initially identified in *Caenorhabditis elegans* as an evolutionary conserved RNA-binding protein that plays an essential role during development (1). In mammals, Lin28 is widely distributed during embryonic maturation, but its expression becomes restricted to specific tissues in adulthood (2). Demonstration of Lin28 expression in embryonic stem cells supported its putative role as a pluripotency factor; a function that was further documented by the fact that Lin28 was used, together with OCT4, SOX2, and NANOG, for reprogramming adult human somatic cells into induced pluripotent stem (iPS) cells (3).

Two Lin28-related genes, corresponding to *Lin28* (also termed *Lin28a*) and *Lin28b*, have been described in mammals (4–6). Lin28 proteins are post-transcriptional regulators of different targets, by virtue of their RNA-binding activity. Prominently, Lin28 proteins have been shown to bind to the terminal loops of the precursors of microRNAs (miRNAS) of the let-7 family, thereby blocking their processing into mature miRNAs (7). In addition, direct interactions of Lin28 proteins with some conventional mRNAs have been documented, including those encoding IGF2 (5, 8), the pluripotency factor, OCT4 (9), and histone H2a (10), as well as several cell cycle regulators, such as cyclin A and B

and cdk4 (11). All in all, their ability to bind and regulate both miRNAs and conventional mRNAs provides a wide spectrum of putative targets and regulatory actions to Lin28 and Lin28b.

Despite the general assumption that Lin28 and Lin28b have similar targets and are functionally redundant, conclusive demonstration of their relative roles has remained elusive. Indeed, most studies on Lin28 expression have actually targeted Lin28a, whereas little information is available on the expression pattern and eventual functions of Lin28b. Much excitement has been raised recently by genome-wide association studies that have conclusively shown associations between changes in or around the Lin28b locus and the age of menarche in humans (12–16). In good agreement, overexpression of Lin28 in mice has been recently shown to delay puberty onset (17). Notably, despite some degree of similarity, Lin28 and Lin28b appear to have dissimilar patterns of distribution in embryonic tissues (18), an observation that raises the possibility, which is yet to be validated, of partially distinct, nonoverlapping roles of Lin28 and Lin28b during development.

The mammalian testis comprises two different, but closely related, tissue compartments: the interstitial space and the seminiferous tubules. These compartments reflect the two essential functions of the male gonad, namely, the hormone synthesis, mainly testosterone by interstitial Leydig cells, and the formation of male gametes (spermatogenesis) in the seminiferous epithelium. Spermatogenesis is a complex, highly synchronized process whereby undifferentiated germ cells are transformed into mature spermatozoa, through a series of key cellular events including self-renewal of spermatogonial stem cells, meiotic divisions of spermatocytes, and final differentiation of haploid spermatids into highly specialized spermatozoa. In brief, type A spermatogonia constitute the most primitive germ cells. They can be found as single (A_s) cells that, by successive mitotic divisions, give rise to paired (A_{pr}) and chains of aligned (A_{al}) spermatogonia that are interconnected by cytoplasmic bridges as a result of incomplete cytokinesis (19, 20). The A_{al} spermatogonia undergo specific differentiation to become type A1 spermatogonia that, through concomitant mitotic divisions and differentiation at specific stages of the seminiferous epithelial cycle, produce A2, A3, A4, intermediate (In) and B spermatogonia. Although A_{pr} and A_{al} spermatogonia are undergoing incipient differentiation, as they are functionally committed to further progress into type A spermatogonia (21), they are usually termed undifferentiated spermatogonia (22), in contrast to the more advanced type A–B spermatogonia that display stage-dependent proliferative activity and progressive differentiation. Division of B spermatogonia into spermatocytes initiates meiosis and after two meiotic divisions gives rise to haploid spermatids. Then, a final complex differentiation process, involving extensive chromatin remodeling related to nuclear condensation and sex-specific genomic imprinting, as well as morphological changes such as acrosome and tail formation, transforms round spermatids into one of the most specialized cells in the body, ie, the male gamete. As spermatogenesis proceeds through a series of sequential steps, tightly regulated patterns of expression, affecting genes/proteins with specific roles in the unique cellular processes involved in gametogenesis, become activated or repressed, under the regulation of both transcriptional and translational mechanisms.

Among its different genetic and epigenetic regulators, recent evidence has documented that miRNAs, as small noncoding RNAs with ability to post-transcriptionally regulate (mainly inhibit) gene expression, are likely to play essential roles in the control of spermatogenesis (23–26). Accordingly, up-stream regulators of miRNA synthesis have been studied as potential modulators of spermatogenesis (27). In this context, Lin28 has been found to be differentially expressed in mouse, and more recently primate, spermatogonia and suggested to play a role in the maintenance of spermatogonial stemness (27, 28), as well as in the development of germ cell tumors (29). Indeed, despite its wide expression during embryonic development, the testis is one of the few tissues where the presence of Lin28 has been demonstrated in adulthood in the mouse, hamster, marmoset monkey, and human (27, 28), as well as in testicular germ cell cancers (30, 31). These analyses have selectively targeted Lin28a, whereas the expression and potential regulation of Lin28b remain virtually unexplored. We provide herein a detailed comparative analysis of the patterns of expression and distribution of Lin28a (termed hereafter as Lin28) and Lin28b in the mouse testis, during postnatal development and in adulthood; the latter, in relation to the different phases of spermatogenesis. In addition, in order to gain functional insight of our data, our studies were extended to expression analyses of *let-7a* and *let-7b* miRNAs in selected experimental groups, and included also the assessment of changes in the testicular patterns of RNA expression and protein distribution of Lin28 and Lin28b, as well as of *let-7a* and *let-7b* miRNAs, both in basal conditions and after gonadotropin treatments, in a mouse model of congenital hypogonadotropic hypogonadism with severe spermatogenetic arrest because of genetic inactivation of the kisspeptin receptor, Gpr54 (32).

Materials and methods

Experimental animals and tissue processing

Testes from male mice at day 1, day 4, day 7, day 10, day 15, day 21 postpartum, as well as young adult (2-month-old) mice from the C57B/6 strain (n = 3–5 animals per age-point) were dissected upon decapitation of the animals and fixed overnight in Bouin for immunohistochemical (IHC) analyses. In addition, testicular samples from mice at day 1, day 15, and day 45 postpartum ($n \geq 6$–7 animals per age-point) were obtained following decapitation and frozen in liquid N_2 until use for RNA/miRNA analyses. For IHC studies, the samples were washed and dehydrated through graded ethanol, were cleared in xylene, and embedded in paraffin. Five μm-thick cross-sections were cut and placed on poly-L-lysine-coated slides and used for IHC. Some testes were cut longitudinally. This provides nearly longitudinal sections of the seminiferous tubules to facilitate stage identification by taking advantage of the succession of the stages of the seminiferous epithelium along the tubules. Some sections were stained with PAS or hematoxylin and eosin. Identification of the stages was based on previously published criteria (33). The above experimental procedures (tissue dissection following decapitation) were conducted under the approval of the Cordoba University Ethical Committee for animal experimentation (references 523/24/01/2011 and 2150/09/03/2010), and conducted in accordance with the European Union normative for care and use of experimental animals.

In addition, testicular RNA/miRNA and IHC analyses were conducted in a mouse model of congenital hypogonadotropic hypogonadism as a result of genetic inactivation of Gpr54 (Gpr54 KO), generated in a C57B/6 background; detailed description of the generation and phenotypic characteristics of the Gpr54 KO mouse line used in this study has been recently provided elsewhere (32). Wild-type (wt) animals, harboring two alleles for Gpr54, served as controls. Testicular IHC analyses were conducted at different stages of postnatal maturation, with the following distribution: 7-day, 10-day, 15-day, 21-day, and >2-month-old wt mice; 7-day, 21-day, and >2-month-old Gpr54 KO mice. In addition, RNA/miRNA assays were implemented in testicular samples from adult (>2-month-old) wt and Gpr54 KO mice. Finally, IHC assays for Lin28 and Lin28b were implemented in testicular samples from Gpr54 null mice after standard protocols of gonadotropin priming, as adapted from previous literature (34, 35). In detail, groups of Gpr54 KO mice (n = 4) were subjected to daily administration of recombinant hCG (12.5 IU/rat; Ovitrelle, Merk-Serono, Feltham, United Kingdom) or FSH (3.75 IU/rat; Gonal-F, Merck-Serono) for 7 days. Sampling and processing of testicular tissues for IHC/RNA analyses were conducted as described above.

Testicular morphometric analysis

When relevant, the mean tubular diameter was determined by measuring the diameter of at least 50 tubular profiles per animal under the microscope in hematoxylin/eosin stained sections. The minimum diameter was used as end-point in our analyses because it is not affected by obliquity of the tubular sections. In addition, the density of type A spermatogonia was determined by counting the number of Lin28 immunoreactive (IR) cells per high-power microscopic field (×40 objective, equivalent to an area of 0.1046 mm^2), in a minimum of 25 microscopic fields per animal.

Immunohistochemistry (IHC)

Lin28 and Lin28b protein distribution in the mouse testis was evaluated by IHC, following previously established procedures, using specific antibodies against each target: anti-Lin28 from Abcam (dilution 1:200), and Lin28b-specific polyclonal antibody from ProteinTech Group, Inc (Chicago, Illinois; dilution 1:25). In brief, sections were dewaxed, incubated in 2% hydrogen peroxide in methanol to quench endogenous peroxidase, and after rehydration in graded ethanol, rinsed in PBS. Antigen retrieval (by autoclaving at 1.5 atm for 5 minutes in 0.1M, pH 7.6 citrate buffer) was necessary for Lin28 immunostaining. Thereafter, sections were incubated overnight with primary antibodies. Bound antibodies were revealed by the avidin-biotin-peroxidase complex method, as specified by the manufacturer (Vector Laboratories, Burlingame, California). Tissue samples from different ages were run in the same assays to assess age-related changes in the intensity of immunostaining, which was estimated by two independent observers, using a semiquantitative scale. Negative control sections were run in

parallel by replacing primary antibodies by nonimmune serum or PBS. Immunostained sections were counterstained with hematoxylin and examined under the microscope.

Qualitative final time RT-PCR

Total RNA was isolated from a panel of adult mouse tissue samples using the Trizol reagent (Invitrogen, Paisley, United Kingdom), following the instructions of the manufacturer. Expression of Lin28 and Lin28b genes was assayed by final-time RT-PCR, using the iCycler iQ Thermal Cycler (Bio-Rad Laboratories, Hercules, California). For amplification of the targets, 2 μg of total RNA per tissue sample were treated with RQ1 RNAse-free DNAse-I (Promega, Madison, Wyoming) and retro-transcribed (RT) in a 30 μl reaction, using AMV reverse transcriptase and random primers (Promega). General conditions for PCR were as described elsewhere (36). The PCR cycling conditions of Lin28 and Lin28b transcripts were as follows: initial denaturation and enzyme activation at 95°C for 5 minutes, followed by 34 cycles of denaturation at 95°C for 30 seconds, annealing at 63°C for 30 seconds, and extension at 72°C for 15 seconds. The primer pairs used were: Lin28-forward: 5′-GTCTTTGTGCACCAGAGCAA-3′ and Lin28-reverse: 5′-CTTTGGATCTTCGCTTC TGC-3′ (amplicon size: 194-bp); Lin28b-forward: 5′-TGGTTCAAC-GTGCGCATGGGA-3′ and Lin28b-reverse: 5′-CCACTGGCTCTCCTTCTTTCAAGCT-3′ (amplicon size: 145-bp). As internal control, amplification of a 290-bp fragment of L19 ribosomal protein mRNA was carried out in parallel in each sample, using cycling conditions similar to those described above (except for an annealing temperature of 55°C) and the following primer pair: RP-L19 forward: 5′-GAAATCGCCAATGCCAACTC- 3′ and RP-L19 reverse: 5′-ACCTTCAGG TACAGGCTGTG-3′.

Quantitative real-time PCR

Total RNA was extracted from the different testis specimens (see above) using Trizol reagent (Invitrogen). Quality and concentration of the RNA were determined by spectrophotometer, ND-1000 NANODROP (Thermo-Scientific, Wilmington, Delaware). Real-time PCR was performed on a Roche 480 real-time PCR instrument.

For Lin28 and Lin28b mRNA quantification in testis samples from different age-points or genotypes, 1 μg RNA was used for cDNA synthesis following the protocol of M-MLV. For PCR, we used SYBR Green qPCR Master Mix (Promega) with the following primer sequences: Lin28-forward/Lin28-reverse: as described above; Lin28b-forward/Lin28b-reverse: as described above; HPRT-forward: 5′-CAGTCC-CAGCGTCGTGAT-3′, HPRT-reverse: 3′-AGCAAGTCTTTCAGTCCTGTC-5′; S11 forward: 5′-CATTCAGACGGAGCGTGCTTAC-3′, reverse: 5′-TGCATCTTCATC TTCGTCAC-3′. PCR was initiated by one hold of 95ºC for 10 minutes, followed by 40 cycles of 15 seconds at 95ºC, 35 seconds at 63ºC, and 5 seconds at 72ºC, followed by one hold of 72ºC for 10 minutes. HPRT and RP-S11 served as the internal reference; relative Lin28 and Lin28b mRNA levels were normalized using the geometric mean of expression of these two reference transcripts.

For miRNA quantification, *let-7a* and *let-7b* were selected as representative of the let-7 family; they being encoded by two different clusters (37). cDNA was synthesized by using 10 ng total RNA with TaqMan–specific RT primers and the TaqMan microRNA reverse transcription kit (Applied Biosystems, Foster City, California). Thereafter, quantitative rt PCR was performed using predesigned assays for *let-7a*, *let-7b*, and *RNU6* (Applied Biosystems). PCR reactions were carried out as follows: 50ºC for 2 minutes, 95ºC for 10 minutes, followed by 40 cycles of 95ºC for 15 seconds and 60ºC for 1 minute. For quantitative miRNA determination, RNU6 gene served as internal reference.

Statistics

RT-PCR analyses (mRNA and miRNA) were performed in duplicate from at least six RNA samples per group (n = 6 for 1- and 15-day-old groups; n = 7 for 45-day-old group; n = 5 for adult Gpr54 KO and wt mice). For developmental studies, data are expressed as percentage of 1-day-old group and presented as mean ± SEM. For studies in Gpr54 mice, data are expressed as percentage of the wt group and presented as mean ± SEM. Data were analyzed using SigmaStat 3.1 (Systat Software, Inc., Chicago,

Illinois). Statistical significance was determined by unpaired Student *t* test or ANOVA followed by post hoc Student Newman Keuls test. $P < .05$ was considered significant.

Results

Screening of adult mouse tissues for expression of *Lin28* and *Lin28b* genes was applied using conventional RT-PCR procedures. This analysis revealed that in the adult mouse, *Lin28* is only prominently expressed in the testis, whereas weak to null expression was detected in a panel of tissues including the pituitary, ovary (both with low but detectable mRNA levels), skeletal muscle, liver, brown adipose tissue, lung, spleen, heart, and hypothalamus. Likewise, *Lin28b* transcript was abundantly expressed in adult mouse testis, yet equally prominent RNA levels were detected in the hypothalamus, whereas modest but detectable expression was observed at the pituitary, skeletal muscle, and (faintly) the ovary. The rest of the tissues included in the panel (see above) were negative for *Lin28b* expression. Representative PCR amplification patterns of *Lin28* and *Lin28b* transcripts in selected tissues, including the testis, hypothalamus, liver, and muscle, are shown in Supplemental Figure I-A (published on The Endocrine Society's Journals Online web site at http://endo.endojournals.org).

In agreement with RNA data, the presence of both Lin28 and Lin28b peptides was confirmed by initial IHC analyses conducted in testes from adult mice. Such studies also disclosed rather disparate cellular locations for Lin28 and Lin28b proteins within the testicular tissue, which set the basis for additional IHC and molecular analyses during postnatal maturation and in a mouse model of hypogonadism (see below). Thus, Lin28 IR was restricted to the seminiferous tubules (Supplemental Figure I-B, D), where the signal was confined to cells at the basal zone of the seminiferous epithelium, thus suggesting expression in premeiotic germ cells. In contrast, interstitial cells were negative (Supplemental Figure I-B, D). Unlike Lin28, Lin28b IR was detected at both the interstitium and seminiferous tubules (Supplemental Figure I-C). In the interstitial compartment, strong cytoplasmic Lin28b IR was observed in Leydig cells (Supplemental Figure I-C, E), whereas other interstitial cells and blood vessels were negative.

Lin 28 and Lin28b expression during postnatal testicular development

Considering the important changes that take place in germ and somatic cell lineages during postnatal testicular development, two complementary approaches were undertaken: (a) IHC analyses were conducted in mouse testis samples obtained at different stages of neonatal and infantile development (between day 1 and day 21 postpartum); and (b) *Lin28* and *Lin28b* mRNA expression was assayed at three representative ages of postnatal testicular maturation (namely, day 1, day 15, and day 45 postpartum). Of note, given the functional auto-regulatory loop between Lin28 and miRNAs of the let-7 family (7), RNA analyses also included expression assays for *let-7a* and *let-7b* levels, as representative of this miRNA family.

IHC analyses confirmed the detection of Lin28 and Lin28b in mouse testis, also at early stages of postnatal maturation. In newborn animals (day 1), germ cells corresponded to gonocytes; these were located at the center of the tubules, showed large nuclei with prominent nucleoli, and were mitotically quiescent. Gonocytes displayed Lin28 immunostaining at both nucleus and cytoplasm (Figure 1-IA), with no obvious difference in terms of signal intensity being detected among different gonocytes. On day 4 postpartum, most gonocytes had migrated to the basal zone of the tubules and showed a high mitotic activity (Figure 1-IB). At this stage, some gonocytes were still present at the center of the tubules, showing nuclear and cytoplasmic Lin28-IR (Figure 1-IB, inset). In addition, spermatogonia displaying weaker Lin28 immunostaining in the nucleus and cytoplasm were also observed in contact with the basement membrane (Figure 1-IB). On day 7 postpartum, gonocytes were no longer found, and germ cells corresponded to type A spermatogonia, which showed frequent mitotic figures and homogeneous (preferential) cytoplasmic Lin28-IR (Figure 1-IC). Meiotic cells were present from day 10 onwards (preleptotene/leptotene spermatocytes on day 10, pachytene spermatocytes on day 15 and day 21, and some early round spermatids on day 21). Clear differences in the intensity of immunostaining among spermatogonia were evident at day 10, with some cells showing strong Lin28-IR (Figure 1-ID). This population of strongly positive spermatogonia for Lin28 was fully established by day 15 (Figure 1-IE), and was clearly detectable on day 21 testes (Figure 1-IF).

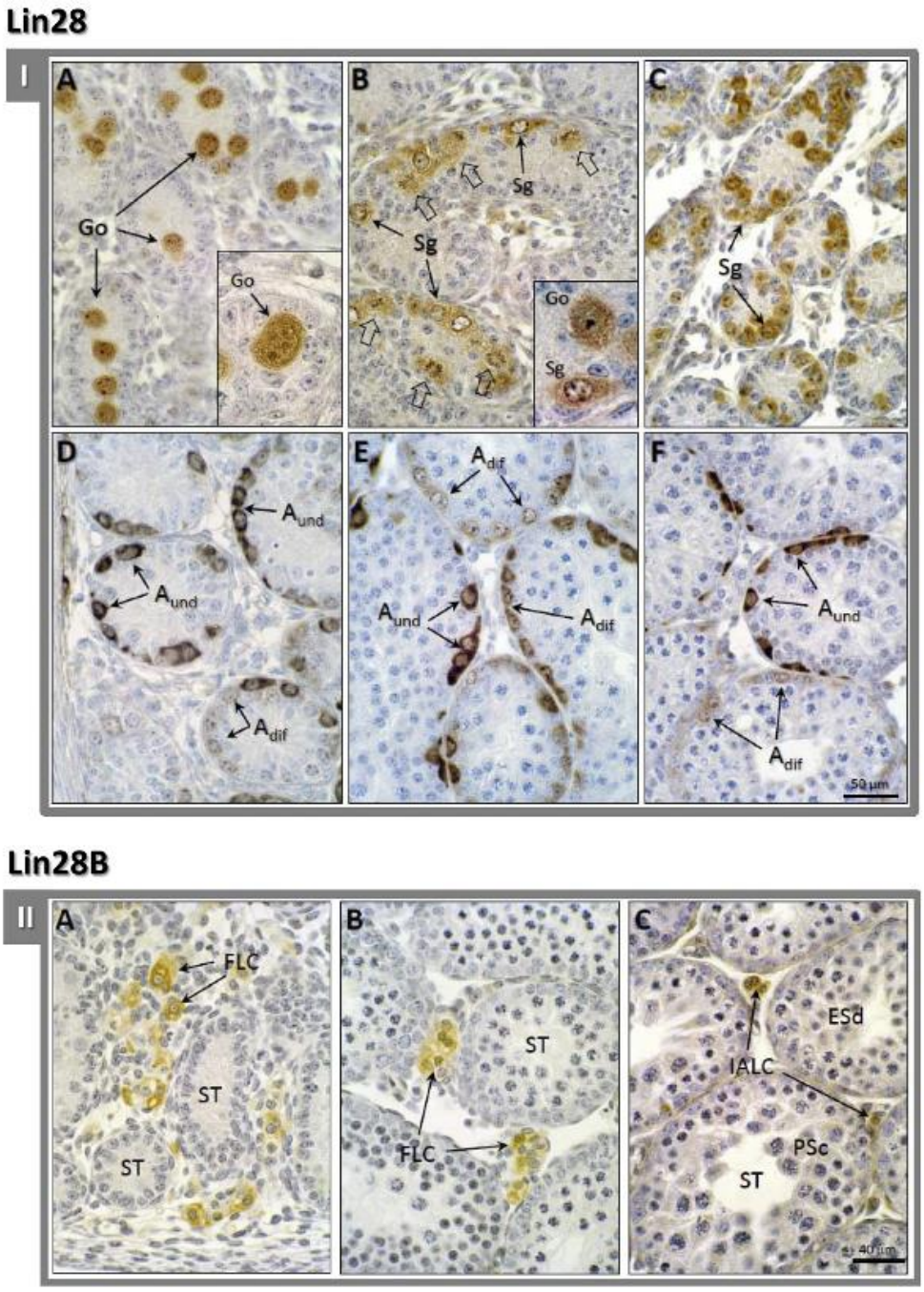

Figure 1. Cellular distribution of Lin28- and Lin28b-IR in mouse testis during postnatal development. In the upper panels (I), IHC analyses of Lin28 are presented. On day 1 postpartum (I-A), gonocytes were located in the center of the tubules and showed nuclear and cytoplasmic Lin28 IR (Go in the inset). On day 4 (I-B), most gonocytes had migrated to the basement membrane and were undergoing mitotic divisions (arrows); the resulting spermatogonia (Sg) showed predominantly cytoplasmic Lin28 immunostaining. On day 7 (I-C), type A spermatogonia were abundant and displayed homogeneous cytoplasmic Lin28 IR. On day 10 (I-D), day 15 (I-E), and day 21 (I-F), two different populations of spermatogonia, as classified in relation to the intensity of Lin28 staining, were clearly identified, and confirmed to correspond to undifferentiated (Aund) and differentiated (Adif) spermatogonia, with string and weak Lin28 IR, respectively. In the lower panels (II), IHQ analyses of Lin28b in mouse testis at different stages of postnatal development are presented. Specific immunostaining was absent in the seminiferous tubules (ST) and was restricted to the interstitial space, where fetal Leydig cells (FLC) were immunoreactive for Lin28b, albeit with different intensities, along the study period (day 1, day 7, day 10, day 15, and day 21 postpartum; see II-A, II-B). In addition, putative, immature adult-type Leydig cell precursors (IALC), as detectable in day 21 testes, were also positive for Lin28b-IR (II-C).

Like our initial adult data, Lin28b immunostaining in postnatal mouse testes was detected in the interstitium, where it appeared restricted to fetal Leydig cells, which were abundant in the interstitial areas during the early postnatal period and whose density decreased thereafter as a consequence of testicular growth (Figure 1-II). Lin28b-positive Leydig cells were detected at all neonatal/infantile ages tested. In fact, Lin28b IR was also observed in presumably immature adult-type Leydig cell precursors, present in the interstitial space of day 21 mouse testes. In clear contrast, no cells showing Lin28b immunostaining were found in the seminiferous tubules of neonatal/infantile mice.

In good agreement with IHC results, expression of Lin28 and Lin28b mRNA was detected in mouse testes at all the age-points selected, corresponding to the neonatal (day 1), infantile (day 15), and pubertal/early adult (day 45) stages of postnatal maturation. However, the profiles of expression across the study-period disparately varied for both signals. Thus, whereas Lin28 mRNA levels abruptly increased (>14-fold increase) between day 1 and day 15 and markedly declined thereafter (~60% reduction between day 15 and day 45), Lin28b mRNA expression increased between the neonatal and infantile periods (~7-fold rise) but remained elevated during the pubertal transition, with relative mRNA levels at day 45 that were similar to those of day 15 (Figure 2A-B). In clear contrast, relative levels of *let-7* miRNAs were maximal in the neonatal mouse testis and declined thereafter. Differences were noted also in the postnatal profiles between *let-7a* and *let-7b*. Thus, whereas *let-7a* levels gradually declined, with 50% reduction between the neonatal and infantile period and further lowering in day 45 samples, *let-7b* expression remained elevated in day 15 testes, whereas it dropped by <60% during the pubertal transition (Figure 2C-D).

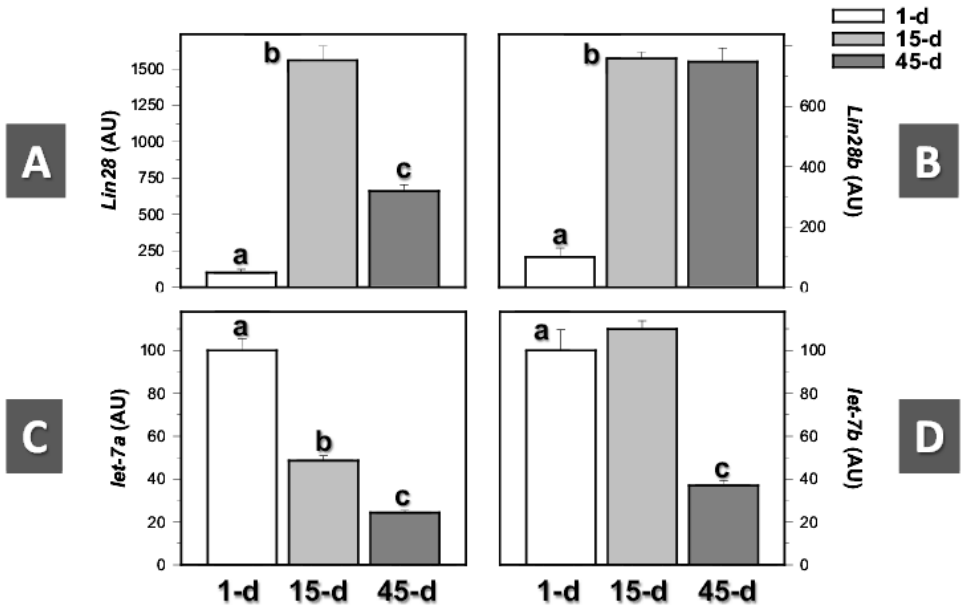

Figure 2. Expression profiles of Lin28 and Lin28b mRNAs in the mouse testis during postnatal maturation. Three representative ages were selected for analysis: day 1 (neonatal), day 15 (infantile), and day 45 (pubertal/ young adult) postpartum. In addition to Lin28 and Lin28b expression (A, B), the relative levels of let-7a and let-7b miRNAs were also detected at the same age-points for comparative purposes (C, D). Bars with different superscript letters are statistically different ($P < .05$ by ANOVA followed by Student-Newman-Keuls multiple range test).

Characterization of Lin28 and Lin28b expression in the adult mouse testis

Detailed IHC analyses of the patterns of Lin28 and Lin28b were also conducted in adult mouse testes. Considering its putative distribution profile, special attention was paid to correlate changes in Lin28 immunostaining with the stages of the seminiferous epithelium. Our studies confirmed that, as was the case in prepubertal testes, cells showing Lin28-IR in adult mouse testis correspond to type A

spermatogonia. Of note, different degrees of intensity of Lin28 IR, beyond the expectable intercellular variability, became apparent within the seminiferous compartment upon evaluation of IHC results, which allowed identification of two major profiles: cells showing very strong cytoplasmic Lin28 immunostaining vs. cells displaying fainter and more diffuse Lin28-IR.

Although the different types of A spermatogonia cannot be discriminated merely by morphological criteria, they follow a specific division pattern during the stages of the seminiferous epithelium (33) that permits overall identification. In this study, all spermatogonia present at stages VII–VIII showed strong cytoplasmic Lin28 immunostaining (Figures 3-IA, B), whereas during stages IX–I, spermatogonia showed either strong or progressively fainter Lin28-IR (Figures 3-IC, D). Furthermore, from stages II–III to stage VI, most spermatogonia lacked Lin28 immunostaining, although strongly positive spermatogonia were also occasionally found. Interpretation of such IHC patterns in the context of the division program of spermatogonia led us to conclude that strong Lin28 immunostaining is characteristic of undifferentiated (A_s, $A_{pr,}$ and A_{al}) spermatogonia, present throughout the stages of the cycle, and differentiating A1 spermatogonia, at stages VII–VIII (Figure 3-IA, B and IIA). In contrast, late differentiating A spermatogonia, corresponding to A2 (at stages IX–XI; see Figure 3-IIB), A3 (at stage XI–I; see Figure 3-IC, D and II-C), and A4 (at stages I–II; see Figure 3-IID) spermatogonia, showed progressively fainter Lin28-IR. On the other hand, at stages III-VI, both In (Figure 3-IIE) and B (Figure 3-IIF) spermatogonia lacked Lin28 IR, although occasional strongly stained undifferentiated A spermatogonia were also found at these stages (Figures 3-IIB, C).

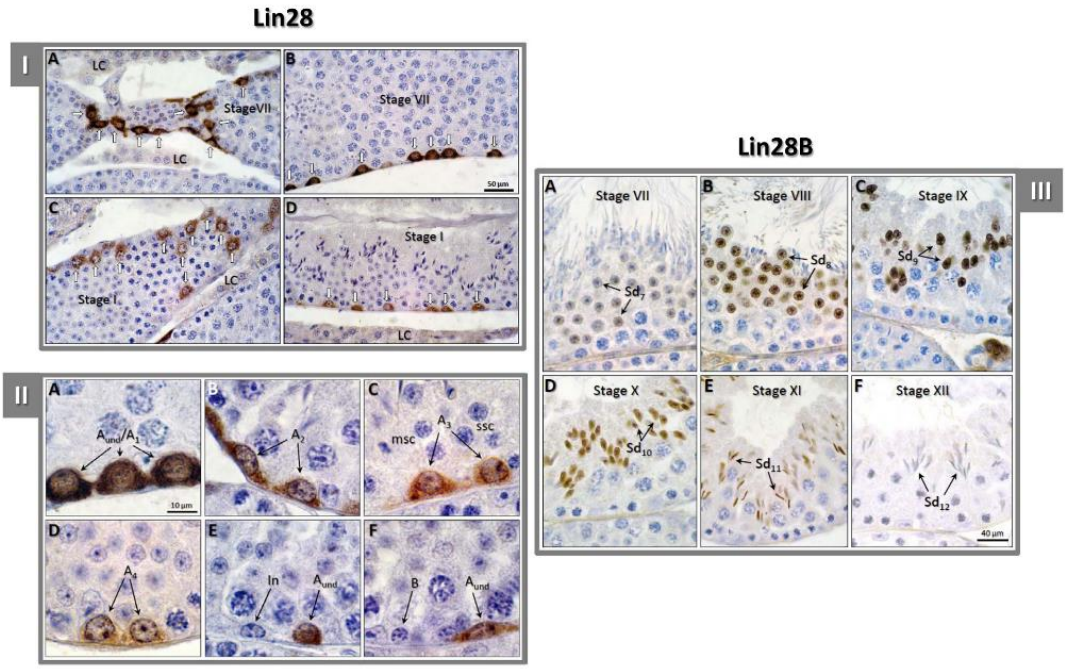

Figure 3. Cellular distribution of Lin28 and Lin28b in the adult mouse testis. In the upper-left panels (I), tangential (I-A, I-C) and longitudinal (I-B, I-D) sections of seminiferous tubules are presented; spermatogonia are indicated by arrows. All spermatogonia present at stage VII (I-A, I-B), corresponding to either As, Apr, Aal, or A1 spermatogonia displayed strong Lin28-IR. In stage I (I-C, I-D), most spermatogonia, corresponding to A3/A4 spermatogonia showed a fainter staining, whereas interstitial Leydig cells (LC) did not show any detectable Lin28-IR. Further details of the distribution of Lin28-IR in adult mouse spermatogonia are provided in the lower-left panels (II). Undifferentiated (Aund) or A1 spermatogonia at stage VII (II-A), showing strong immunostaining are shown. In addition, the progressive decrease in Lin28-IR intensity is also documented in A2 spermatogonia at stage X-XI (II-B), A3 spermatogonia in stage XII (II-C), and A4 spermatogonia at stage I-II (II-D). In stage XII, secondary spermatocytes (ssc) and meiotic spermatocytes (msc), without Lin28 staining, are also shown. Intermediate (In) spermatogonia at stages II-IV (II-E) and B spermatogonia at stages IV-VI were negative. Sporadic undifferentiated (Aund) spermatogonia, positive for Lin28b, were found at stages III-VI (II-E, II-F). Finally, the pattern of cellular distribution of Lin28b-IR in the adult mouse testis is documented in the right panels (III). Round spermatids (Sd7) at stage VII displayed variable immunostaining, ranging from barely detectable to faint (III-A), whereas strong IR (Sd8) was detected at stage VIII (III-B). Strong Lin28b staining was also present in elongating spermatids (Sd9-11), from stage IX to stage XI (III-C to III-E), whereas Lin28b-IR disappeared in elongated spermatids (Sd12) at stage XII (III-F).

In good agreement with our initial data, Lin28b IR was also observed in the seminiferous compartment of the adult mouse testis. Within the seminiferous tubules, Lin28b immunostaining was nuclear, showed a stage-specific pattern, and was confined to postmeiotic spermatids during the nuclear elongation phase. Thus, round spermatids at stage VII showed variable Lin28b-IR, ranging from barely detectable to faint signals (Figure 3-IIIA), whereas elongating spermatids from stage VIII to stage XI showed strong nuclear immunostaining that abruptly disappeared at stage XII (Figures 3-IIIB, F) and was absent thereafter. Note that, in addition to its seminiferous expression, Lin28b IR was also detected in the interstitial compartment of adult mouse testis, with strong cytoplasmic staining in mature adult-type Leydig cells (Supplemental Figure I-C, E).

Testicular expression of Lin28 and Lin28b in a mouse model of hypogonadotropic hypogonadism

Protein and RNA studies of the Lin28/Lin28b system were also implemented in testes from a mouse model of congenital hypogonadotropic hypogonadism, as a result of inactivation of Gpr54 (32). This mouse line displays markedly decreased circulating LH and FSH levels, as well as severely reduced testis weights in adulthood (6.6 ± 0.6 mg in Gpr54 KO vs 91.5 ± 1.7 mg in wt mice; $P < .01$), thus demonstrating its hypogonadal state of central origin (32). Detailed morphometric analyses in adult wt mice showed normal seminiferous tubules with complete spermatogenesis and prominent eosinophilic Leydig cells in the interstitial areas (Supplemental Figure II-A). Like in our studies in C57B/6 adult mice (*see above*), IHC analyses of Lin28 showed strongly immunoreactive type A spermatogonia located at the base of the seminiferous epithelium (Supplemental Figure II-B). In addition, both Leydig cells in the interstitial areas and elongating spermatids within the seminiferous tubules showed intense Lin28b-IR. In contrast, adult Gpr54 KO mice showed small seminiferous tubules with arrested spermatogenesis; the most advanced germ cells corresponded to leptotene (or occasional pachytene) spermatocytes (Supplemental Figure II-C). In Gpr54 null mice, Lin28-positive type A spermatogonia were present, but showed some irregular distribution throughout the testicular sections (Supplemental Figure II-D). In contrast, Lin28b immunostained cells were absent, because of the lack of elongating spermatids and differentiated Leydig cells (data not shown).

In wt mice, the density of gonocytes/type A spermatogonia displaying discernible Lin28-IR raised from 1 to 10/15 days postpartum, despite the parallel increase in tubular diameter, because of the proliferative activity of these cell types (evidenced by frequent mitotic figures; see Figure 4-I), but it decreased rapidly from 15 days onwards, because of the enlargement of tubular volume. In Gpr54 null mice, tubular diameter and the density of A spermatogonia were equivalent to those of wt mice at 7 days postpartum. Thereafter, the mean tubular diameter failed to expand significantly, in contrast to wt animals, and a decrease in type A spermatogonia density was observed at 21 days and >2 months postpartum. However, because of the lack of increase in tubular diameter, the tubular density of Lin28-IR type A spermatogonia in Gpr54 KO mice was higher than in wt mice at both age-points. The absolute decrease in density in Gpr54 KO mice was likely because of decreased proliferation and/or increased cell death. In fact, high cell death rates of A spermatogonia in testes from Gpr54 KO animals is suggested by the frequent observation of numerous tubular sections lacking type A spermatogonia, and consequently germ cells (Figure 4-II). In clear contrast, isolated tubular sections lacking type A spermatogonia were only occasionally found in wt mice.

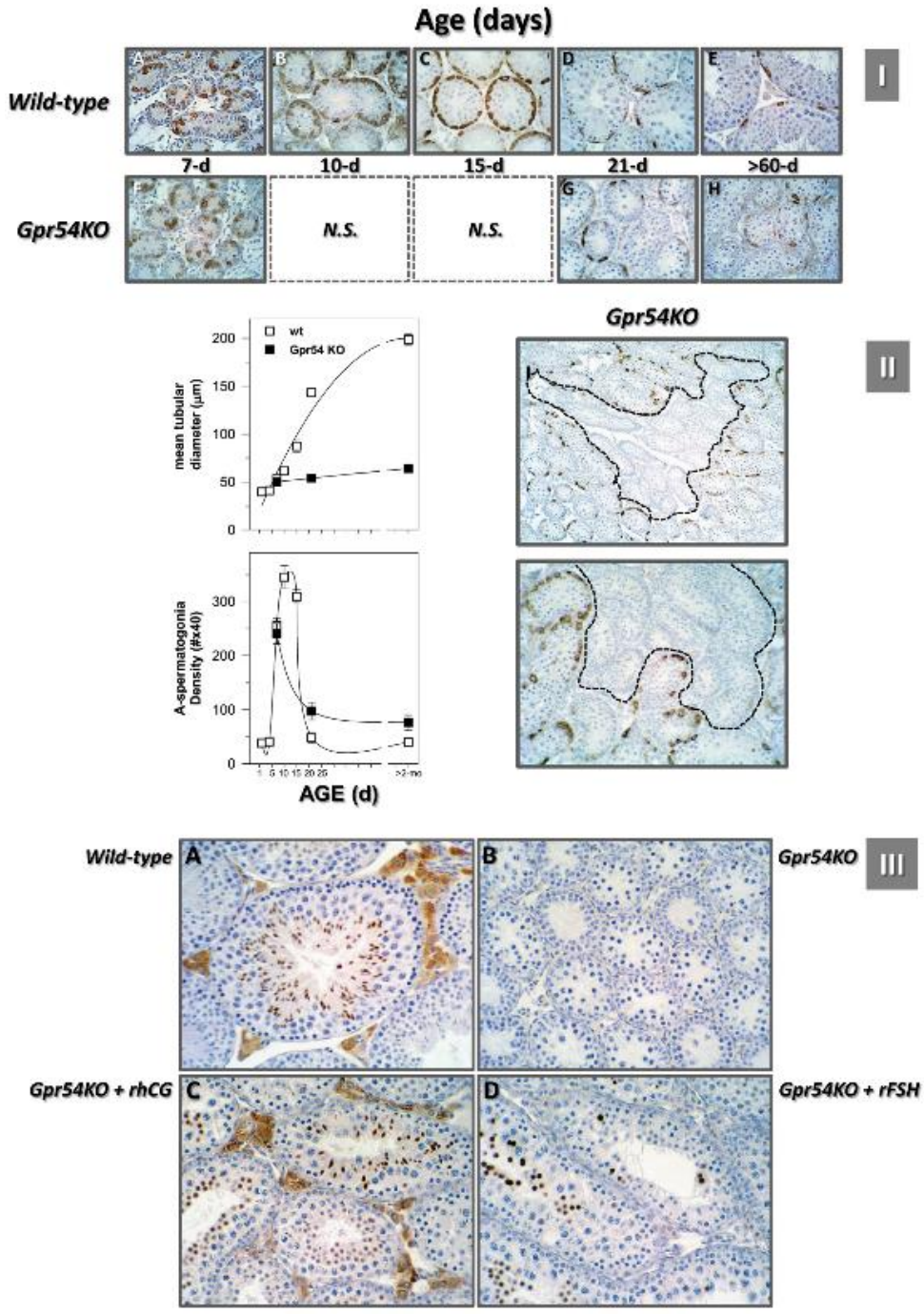

Figure 4. IHC analyses of Lin28 members in the testes of Gpr54 KO mice during postnatal maturation and after gonadotropin treatment. The Gpr54 null mouse is a model of congenital hypogonadism of central origin, as a result of genetic inactivation of the kisspeptin receptor, Gpr54. Wild-type (wt) mice, harboring two alleles of Gpr54, served as controls. In the upper panels (I), IHC studies of Lin28 in testes from wt and Gpr54 null mice at different stages of postnatal development are shown (wt mice, A: 7-d, B: 10-d, C: 15-d, D: 21-d, E: >60-d; Gpr54 KOs, F: 7-d, G: 21-d, H: > 6-d). Note that because of limited availability of KO animals, the postnatal ages, 10 days and 15 days, were not studied in the latter (N.S.). In addition to representative images of Lin28-IR at different postnatal ages, quantification of the changes in mean tubular diameter and Lin28-positive type A spermatogonia density across postnatal maturation in the testes from wt and Gpr54 KO mice are presented in the middle panels (II). Similarly, representative testicular sections from Gpr54 null mice, showing tubular segments devoid of Lin28-IR type A spermatogonia (marked by dotted lines), are also displayed in this panel. In addition, in the lower panels (III), IHC analyses of Lin28b in the testes of adult wt and Gpr54 KO mice are presented. In addition, groups of null mice were treated for 7 days with effective doses of recombinant hCG (as superagonist of LH) or FSH, and representative testicular sections stained for Lin28b are also shown in panel C (Gpr54 KO+ rhCG; D: Gpr54 KO+rFSH). Note that because gonadotropin treatments failed to substantially alter the pattern of Lin28 in Gpr54 KO mouse testes, no representative images of Lin28 IHC are shown in this figure.

To provide an insight into the hormonal regulation of the testicular expression patterns of Lin28 and Lin28b, IHC analyses were also implemented in Gpr54 null mice, subjected or not to protocols of gonadotropin priming, involving isolated expression of recombinant hCG or FSH, as previously described. Considering that Lin28 IR was persistently detectable in the testes of Gpr54 KO mice, but Lin28b was absent, major efforts were devoted to map changes in the expression profiles of the latter following effective gonadotropin stimulation. As shown in Figure 4-III, treatment with hCG for 7 days resulted in a marked increase in the seminiferous tubule diameter, with progression of spermatogenesis up to elongating spermatids, and enlargement of interstitial Leydig cells. In turn, repeated FSH administration resulted in a detectable, although less prominent, increase in tubular diameter and progression of spermatogenesis up to the round spermatid stage, without any discernible effect on the morphology of Leydig cells. In agreement with our initial analyses (see above), in wt mice both Leydig cells and (mainly elongating) spermatids displayed robust Lin28b-IR (Figure 4-IIIA); in contrast, Gpr54 null mice failed to show detectable Lin28b immunostaining (Figure 4-IIIB). This was rescued by gonadotropin administration, with different effects being observed between hCG and FSH treatments. Thus, whereas hCG administration induced very intense Lin28b-IR in Leydig cells and elongating spermatids (Figure 4-IIIC), repeated FSH injections caused more modest effects, with Lin28b signals being detected in round spermatids, but not in Leydig cells (Figure 4-IIID). Notably, testicular Lin28-IR did not change substantially after gonadotropin treatment of Gpr54 null mice, with a persistent pattern of expression in undifferentiated and type A spermatogonia (data not shown).

Complementary RNA analyses, assessing changes in testicular *Lin28/let-7* levels between wt and Gpr54 KO mice, were also implemented in adult animals. As shown in Figure 5, null mice displayed increased relative levels of Lin28, but not Lin28b, mRNA in the testes, with ~3-fold increase over wt values. In addition, Gpr54 null mice showed enhanced relative levels of *let-7a* (~2.5-fold increase) and *let7-b* (~6-fold increase) miRNAs over corresponding wt values. Of note, because testicular weights of null animals were severely decreased vs wt values (~14-fold decrease), besides relative expression (Figure 5), total expression levels of the above targets per testis, as estimated by the product of the expression of the specific transcript by the testicular weight, were calculated. This analysis revealed that total testicular expression of *Lin28/let-7* transcripts was markedly reduced in Gpr54 KO mice, although the degree of suppression varied among the different targets. Thus, total expression levels were 25% (*Lin28*), <8% (*Lin28b*), 17% (*let-7a*), and 43% (*let-b*) of corresponding values in wt mouse testes. Note that this procedure of calculation of total testicular expression of RNAs allows an easy estimation of the absolute expression of a given target per testis and has been previously used by our group to complement relative expression data in models, such as hypophysectomy, characterized by dramatic changes in weight and/or cellular composition of the testis (35).

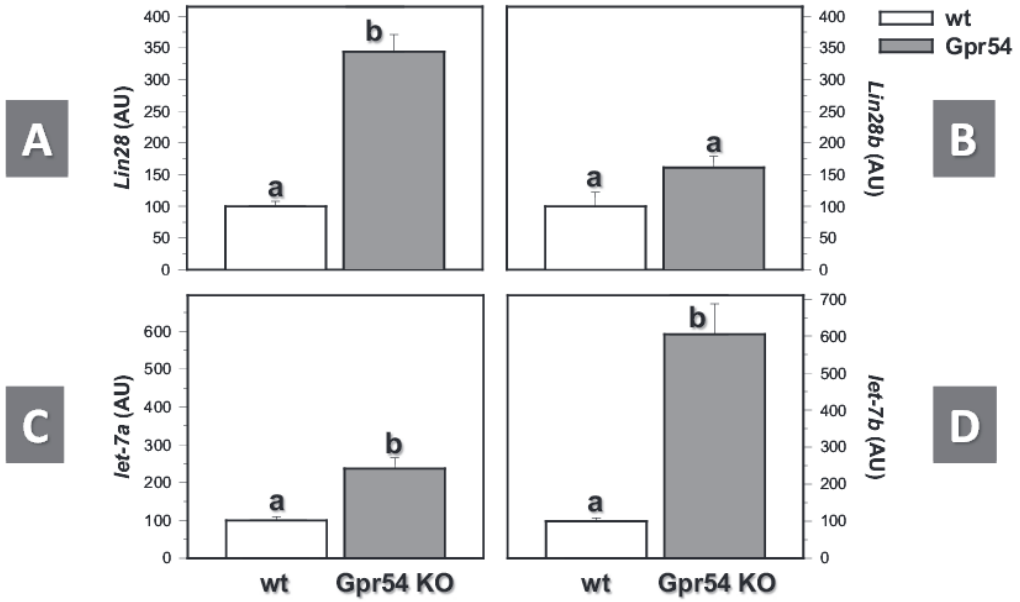

Figure 5. Expression profiles of Lin28 and Lin28b mRNAs in the testis of adult Gpr54 KO mice. The Gpr54 null mouse is a model of congenital hypogonadism of central origin, as a result of genetic inactivation of kisspeptin signaling. Wt mice, harboring two alleles of Gpr54, served as controls. In addition to Lin28 and Lin28b expression (A, B), the relative levels of let-7a and let-7b miRNAs were also detected at the same age-points for comparative purposes (C, D). Bars with different superscript letters are statistically different ($P < .05$ by Student t test).

Discussion

Spermatogenesis is a complex phenomenon, involving numerous cell types and a large array of specific regulatory factors, which act at the transcriptional or post-transcriptional levels and are essential for the fine control of male gametogenesis. Among the post-transcriptional regulatory mechanisms, the putative roles of RNA-binding proteins and miRNAs have been recently suggested, and expression of Lin28, a putative inhibitor of the synthesis of mature *let-7* miRNAs, has been documented in the adult rodent testis (27). Our present study extends and refines those previous observations, as it provides the first systematic analysis of the patterns of RNA expression and protein distribution of Lin28 and the related Lin28b in the mouse testis, during postnatal maturation and in adulthood. Importantly, our data are the first to conclusively demonstrate that Lin28 and Lin28b display distinct RNA expression profiles along postnatal maturation and totally different distribution patterns of the corresponding RNA-binding protein, which were not overlapping in terms of tissue compartments (germ cells vs. interstitial cells), stages and cell types within the seminiferous epithelium (spermatogonia vs spermatids), and even preferential intracellular location (cytoplasmic vs nuclear). These striking findings, which have remained overlooked probably because of the lack of specific studies on Lin28b in the gonads, reinforce the view that Lin28 and Lin28b are likely to conduct different, nonredundant roles in the regulation of male gametogenesis and gonadal function during postnatal maturation.

Previous reports had documented the expression of Lin28 in diverse embryonic tissues, including embryonic stem and primordial germ cells, as well as in adult germ cell tumors (9, 29). Recently, expression of Lin28 has been reported in the adult mouse testis, as to be restricted to undifferentiated (A_s-A_{al}) spermatogonia whereas, according to that study, Lin28-IR was apparently absent in differentiating (ie, A1-A4) spermatogonia (27). Those previous findings are in partial contrast with our current work, where Lin28 was detectable in all type-A spermatogonia, albeit with different intensity. Whereas methodological issues, regarding the IHC procedure, may account for some of these differences, it is also stressed that findings included in the previous study of Zheng and colleagues indirectly suggest that Lin28 is indeed expressed at least in A1 (differentiating) spermatogonia. This could explain, for instance, why the highest number of Lin28-positive cells was detected at stages VII-VIII (27), where active differentiation into A1 spermatogonia causes a substantial decline of the number of undifferentiated spermatogonia (33, 38). Indeed, our present data are suggestive of a conserved expression, at apparent

high levels, of Lin28 in undifferentiated and A1 spermatogonia, as evidenced by the strong IHC signal in all spermatogonia in stages VII–VIII, which was followed by progressive down-regulation of Lin28 levels during A2 to A4 spermatogonial differentiation. Admittedly, further characterization of Lin28-expressing vs. nonexpressing spermatogonial populations, eg, by the use of selective markers of the differentiation status, might help to further refine the phenotypic profiling of these subpopulations.

The above profile is in good agreement with the putative role of Lin28 in promoting pluripotency and maintaining stemness, a phenomenon that has been related with the capacity of Lin28 to block the maturation of *let-7* miRNAs (39), as well as alternative mechanisms targeting coding mRNAs of other pluripotency factors, such as Oct4 (9), and germ cell markers, such as Stella, Prdm14, and Tex14 (9, 29). Spermatogonial stem cells (SSC) are included among the pool of undifferentiated, isolated A spermatogonia (A_s), and possibly also some paired (A_{pr}) and aligned (A_{al}) A spermatogonia (22, 33). Our results support that murine SSC are Lin28-positive, in line with very recent data from nonhuman primate and human testes (28). Of note, differentiation of A_{al} to A1 spermatogonia at about stage VII (21, 33) is followed by stage-dependent proliferation and differentiation of spermatogonia (from A1 to A4), leading to the generation of In and B spermatogonia at stages II-VI. The progressive decrease in Lin28-IR observed in our study paralleled the progressive differentiation of spermatogonia from undifferentiated/A stage up to A4 stage. However, no significant changes were found during the transition from A_{al} to A1 spermatogonia, and that seems to constitute a checkpoint in spermatogonia regulation (22), thus casting doubts on a specific role of Lin28 in this particular phenomenon. As a side observation, despite the expanding number of germ cell markers described so far (22), very few of them appear to be selectively confined to A spermatogonia; hence, the specificity of Lin28 staining for type A spermatogonia in the adult mouse testis may prove valuable as a selective marker for this cell type.

During postnatal development, the testis undergoes dramatic changes in its microenvironment affecting both germ and somatic cell lineages. Changes in germ cells include the initiation of the first spermatogenic wave and the establishment of the SSC population. This is concomitant with developmental changes in somatic cell types, particularly in Sertoli cells, leading to the establishment of the SSC niche that controls stem cell renewal and differentiation in the adult testis. Although the regulation of these processes is not fully understood, some major features of this maturational process have been exposed recently. In brief, gonocytes, which are mitotically quiescent at birth and located at the center of the tubules, migrate toward the basement membrane and undergo extensive proliferation around postnatal days 2–4 (40, 41), giving rise to two spermatogonial cell types: undifferentiated and differentiating type-A spermatogonia (41). Adult-type A1 spermatogonia differentiate thereafter in a stepwise manner, giving rise to primary spermatocytes at day 10 postpartum, and the completion of the first spermatogenic wave by day 35 (42). SSC are included in the pool of undifferentiated spermatogonia resulting from gonocyte divisions, as indicated by the presence of SSC activity on day 4 to day 5 postpartum (40). Our findings on the patterns of Lin28-IR during early postnatal maturation of the testis may increase understanding (and tracing) of this phenomenon. In this sense, it is noted that gonocytes displayed both nuclear and cytoplasmic Lin28 immunostaining, whereas the transition from gonocytes to spermatogonia (between day 1 and day 4) was characterized by the apparent loss of nuclear immunostaining, which became predominantly cytoplasmic in the different types of spermatogonia. Admittedly, the functional significance of the intracellular localization of Lin28 protein during the gonocyte to spermatogonia transition is yet to be determined.

Undifferentiated A spermatogonia in the adult testis displayed strong cytoplasmic expression of Lin28. Surprisingly, type A spermatogonia resulting from gonocyte divisions and present in the testis around day 4 to day 7 postpartum did not show strong Lin28 IR, but rather a weak and diffuse pattern. Indeed, strongly positive spermatogonia appeared only on day 10 and became predominant from day 15 onwards. This may suggest that the establishment of the adult population of undifferentiated A spermatogonia, which contains SSC, occurs during the second postnatal week in rodents. Functional studies have reported that the number of SSC shows a 6.4-fold increase by 5–12 days postpartum (43). Whereas the precise regulation of Lin28, and its functional role in the control of SSC population, remains largely unknown, our current data demonstrate that both the acquisition of strong Lin28-IR and mRNA expression take place during the neonatal to infantile transition. Whether this developmental switch is involved in the expansion of SSC awaits further investigation.

In contrast to Lin28, Lin28b-IR was found in both somatic (interstitial Leydig cells) and germ (spermatids) testicular cells, and was considerably enriched in the adult testis. Expression of Lin28b mRNA was clearly detected in the infantile testis, and unambiguous Lin28b-IR was observed in fetal-type Leydig cells and immature adult-type Leydig cell precursors, present in day 15 mouse testes. Of note, Lin28b-IR in postmeiotic spermatids was highly specific for the elongation phase of spermiogenesis,

from Sd_7 to Sd_{11} steps, corresponding to stages VII-XI of the seminiferous epithelial cycle. The intertubular variability found in stage VII (ranging from barely detectable to faint) was beyond the expectable intercellular variation and probably related to the considerable duration of this phase (44), therefore suggesting that Lin28b protein expression starts in round spermatids during stage VII. In good agreement, round spermatids at stage VIII showed already strong IR. Similarly, Lin28b abruptly disappeared at stage XII, the period of the cycle when the elongation phase of spermiogenesis is almost completed.

The elongation phase of spermatid differentiation is an essential period in male gamete formation where key maturational events take place. These include the process of chromatin remodeling, which involves the replacement of histones by protamines (45), that ultimately leads to chromatin package and nuclear condensation. The fine regulation of this complex phenomenon requires the expression of an array of specific genes, most of them encoding nuclear proteins (45, 46). Our present data document for the first time the selective expression of Lin28b in the nucleus of elongating spermatids. This restricted pattern of expression is highly suggestive of a putative role of Lin28b in the regulation of gene expression in the haploid male genome, likely via modulation of *let-7* miRNA synthesis. Indeed, regulation of spermiogenesis relies largely on post-transcriptional regulatory mechanisms, and miRNAs have recently emerged as putative modulators of spermatogenesis (23, 47). In this context, the abundant presence of Lin28b in elongating spermatids is coincident with substantial changes in the expression profiles of key proteins, such as the loss of histones and the appearance of a series of basic nuclear proteins, namely, testis-specific HMG (tsHMG), histone H1-like protein in spermatids 1 (Hils1), transition proteins 1 and 2 (TP1 and TP2), and protamine 1 (46, 48). Our present findings open up the possibility that, via *let-7* modulation or other regulatory mechanisms, Lin28b may participate in the modulation of such critical changes in protein expression during spermatid elongation.

Recently, an elegant study by Tong and colleagues has documented the expression patterns of some members of let-7 miRNA family, namely *let-7a*, *let-7c*, and *let-7e*, in the mouse testis and their responses to retinoic acid-induced spermatogonial differentiation (49). Of important note, divergent patterns of cellular distribution of the different members of the let-7 family were reported in that study, with variable expression in premeiotic and meiotic germ cells. For instance, *let-7a* was shown to be preferentially expressed in spermatogonia, whereas *let-7c* and *let-7e* were mainly expressed in spermatocytes. In addition, a weak *let-7a* signal was also observed in some interstitial cells of the adult mouse testis. These results provide some clues for interpretation of our current expression data and support our present findings, showing disparate profiles of *let-7a* and *let-7b* miRNA expression along postnatal maturation. Although the concomitant presence of Lin28, Lin28b, and *let-7* miRNAs in the developing and adult mouse testis is highly suggestive of the existence of a reciprocal Lin28/let-7 feedback regulatory loop (7, 39), which has been indirectly suggested also by functional studies on the impact of retinoic acid deficiency on the testicular expression of these targets (49), the differential patterns of cellular distribution [see (49) and present results] may help to explain the partial lack of inverse correlation between some of the elements of this system at specific developmental stages in the mouse testis. In any event, it is remarkable that in the neonatal testis low expression levels of Lin28/Lin28b were associated with maximal levels of *let-7a* and *let-7b* miRNAs, whereas in adulthood maximal Lin28b mRNA levels were accompanied by significantly suppressed *let-7* miRNA expression. The cellular basis and complete functional relevance of such potential associations merits further investigation.

Analyses in Gpr54 null mice, as model of congenital hypogonadism of central origin as a result of the lack of kisspeptin signaling and, hence, low gonadotropin levels, further supported our findings in control mouse testes. The hypogonadal Gpr54 KO mouse displayed grossly preserved testicular histology during early postnatal development, in good agreement with findings in other models of congenital absence of gonadotropic drive, such as the LH receptor KO (LuRKO) mouse (50). Likewise, the pattern of Lin28-IR was roughly similar in wt and Gpr54 KO testes from neonatal (7 d) mice. However, in line with the overt hypogonadotropism of Gpr54 null mice, these animals showed a clear impairment of testicular maturation at later developmental stages. Thus, Gpr54 KO mouse testes failed to show the prototypical increase in tubular diameter during pubertal maturation, suffered spermatogenic arrest and lacked mature Leydig cells in the testicular interstitium, as described also in previous references (32). Nonetheless, *Lin28* mRNA and protein remained clearly detectable in the testes of Gpr54 null mice, where Lin28-IR was observed in presumable undifferentiated and type A spermatogonia (eventually including SSC), whose appearance and maintenance seem to be independent of gonadotropic stimulation. Indeed, the pattern of cellular expression of Lin28 in Gpr54 KO testes did not change substantially after 1 wk of FSH or hCG replacement, thus supporting the view that its spermatogonial expression is gonadotropin-independent. In clear contrast, Lin28b-IR was undetectable, and its absolute mRNA levels dropped markedly (<8% from

wt values) in the testes of Gpr54 KO mice, likely reflecting the lack of mature Leydig cells and spermatids in this model of congenital hypogonadism, hence suggesting that testicular expression of Lin28b requires a strong gonadotropin drive. In fact, gonadotropin administration to Gpr54 null mice rescued such defective expression, so that hCG treatment induced the appearance of strong Lin28b immunostaining, coincident with the appearance of hyperthropic Leydig cells and elongating spermatids, whereas the effects of FSH replacement were less robust, with Lin28b-IR being detected only in round spermatids. In any event, despite the relative enrichment of *Lin28* mRNA transcript, we cannot exclude the possibility of some degree of defective translation of this transcript into a mature protein, which may explain its irregular pattern of IR detected in some testicular sections. Furthermore, the absolute expression levels of *Lin28* were actually decreased in adult testes from Gpr54 null mice, which may be the result of deregulation of the spermatogenic process, as evidenced by the frequent observation of tubular sections lacking type A spermatogonia, probably because of increased cell death of this population in null animals. Furthermore, comparison of the expression profiles of *Lin28* and *let-7* transcripts between wt and Gpr54 KO testes (Figure 5) reveals clear similarities with changes associated to the maturational transition between infantile and young adult periods (Figure 2), as both Gpr54 KO and immature testes displayed markedly elevated *Lin28*, *let-7b* and, to a lesser extent, *let-7a* levels vs. control adult values, whereas the relative *Lin28b* mRNA levels were not significantly different. These observations provide a molecular signature for the state of testicular immaturity of Gpr54 null mice and help to dissect out the gonadotropin-dependent vs independent regulation of *Lin28* and *let-7* expression in the testis.

In summary, we report here the first comparative analysis of the expression patterns of Lin28 and Lin28b in the mouse testis, both during early postnatal maturation and in adulthood, as well as in a model of congenital hypogonadotropic hypogonadism, with or without gonadotropin replacement; a synoptic compilation and interpretation of our results is provided in Figure 6. Our results document that, contrary to the general assumption that both members of the Lin28 family overlap in terms of expression and cellular functions, Lin28 and Lin28b display clearly distinct patterns of RNA expression and protein distribution, both within the seminiferous epithelium (Lin28: undifferentiated and type A spermatogonia; Lin28b: spermatids) and the interstitial space (only Lin28b, detected in Leydig cells). Such patterns of cellular expression are highly suggestive of specific, nonredundant functions of each Lin28 RNA-binding protein in the testis, which may include not only SSC renewal and spermatogonial differentiation (Lin28), but putatively also regulation of key events in spermiogenesis and, eventually, Leydig cell maturation and/or function (Lin28b). From a more general perspective, our present data emphasize the importance of specific analyses of the selective roles of Lin28 and Lin28b in other tissues and tumors, where they may also play divergent functions, as predicted for the testis on the basis of our current RNA and protein expression data.

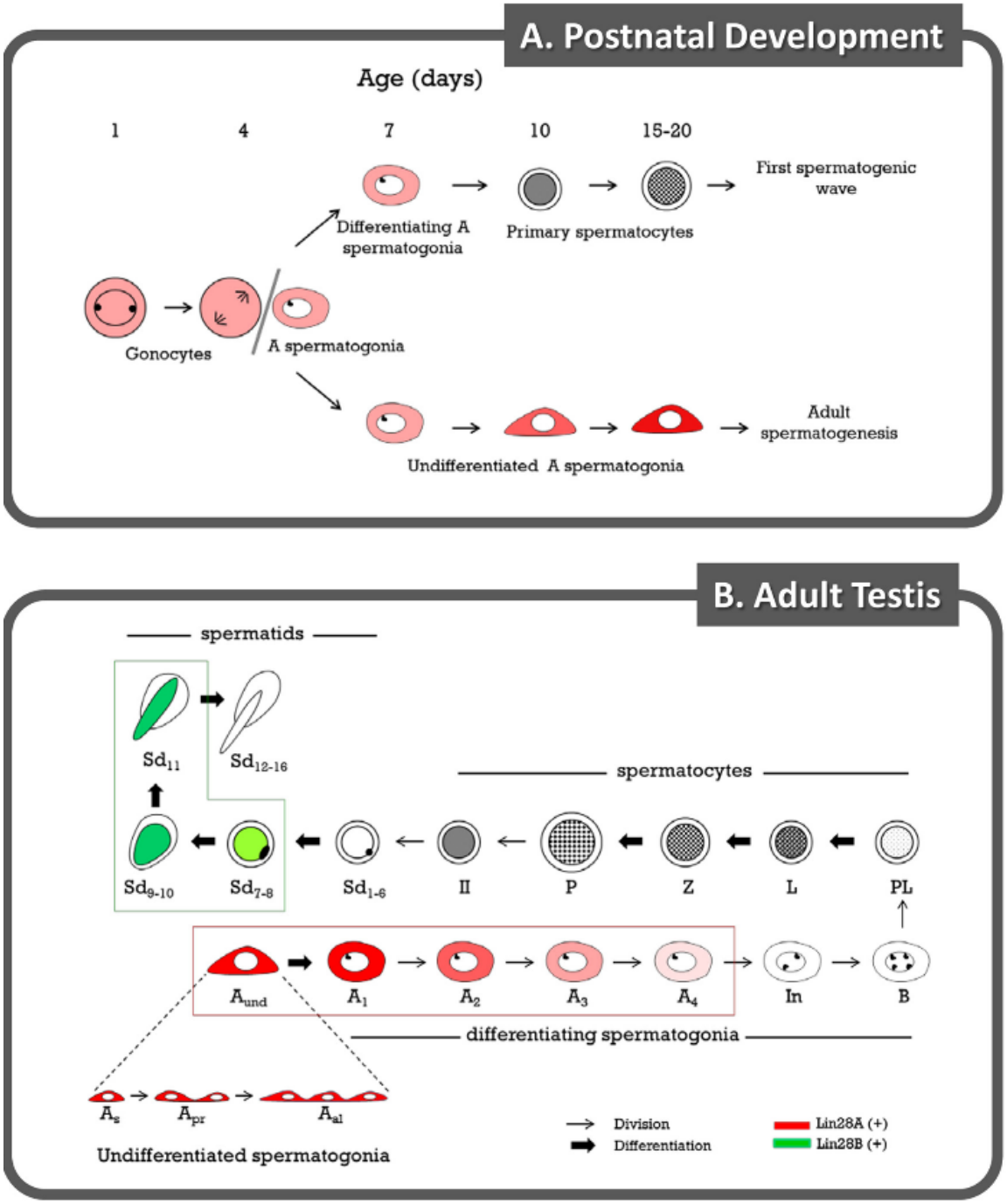

Figure 6. Proposed model for the cellular distribution of Lin28 and Lin28b in the mouse testis during postnatal development and in adulthood. In the upper panel (A), the cellular distribution of Lin28 during postnatal development is schematically depicted. Divisions of gonocytes on day 4 postpartum give rise to two types of spermatogonia: differentiating and undifferentiated spermatogonia. These two types of spermatogonia display a similar pattern of Lin28 IR during the first postnatal week; however, they diverge during the second postnatal week, so that Lin28 IR becomes progressively stronger only in undifferentiated spermatogonia. In addition, in the lower panel (B), a schematic representation is shown of the differential expression patterns of Lin28 and Lin28b protein in germ cells of the adult mouse testis. For further details, see the text.

Abbreviations:
IHC, Immunohistochemic; IR, immunoreactive; RT, retro-transcribed; SSC, spermatogonial stem cell; wt, wild type.

Acknowledgments
The authors thank Desiree Gutierrez Córdoba for superb technical assistance during the conduction of IHC studies. This work was supported by grants BFU 2008-00984 and BFU2011-25021 (cofunded by FEDER EU Program; Ministerio de Ciencia e Innovación, Spain), Project P08-CVI-03788 (Junta de Andalucía, Spain), and EU research contract DEER FP7-ENV-2007-1. CIBER is an initiative of Instituto de Salud Carlos III (Ministerio de Sanidad, Spain).

Disclosure Summary: The authors have nothing to disclose.

References

1. Moss EG , Lee RC , Ambros V. The cold shock domain protein LIN-28 controls developmental timing in C. elegans and is regulated by the lin-4 RNA. *Cell*. 1997;88:637–646.
2. Yang DH , Moss EG. Temporally regulated expression of Lin-28 in diverse tissues of the developing mouse. *Gene Expr Patterns*. 2003;3:719–726.
3. Yu J , Vodyanik MA , Smuga-Otto K , Antosiewicz-Bourget J , Frane JL , Tian S , Nie J , Jonsdottir GA , Ruotti V , Stewart R , Slukvin II , Thomson JA. Induced pluripotent stem cell lines derived from human somatic cells. *Science*. 2007;318:1917–1920.
4. Moss EG , Tang L. Conservation of the heterochronic regulator Lin-28, its developmental expression and microRNA complementary sites. *Dev Biol*. 2003;258:432–442.
5. Balzer E , Moss EG. Localization of the developmental timing regulator Lin28 to mRNP complexes, P-bodies and stress granules. *RNA Biol*. 2007;4:16–25.
6. Guo Y , Chen Y , Ito H, et al.. Identification and characterization of lin-28 homolog B (LIN28B) in human hepatocellular carcinoma. *Gene*. 2006;384:51–61.
7. Viswanathan SR , Daley GQ. Lin28: A microRNA regulator with a macro role. *Cell*. 2010;140:445–449.
8. Polesskaya A , Cuvellier S , Naguibneva I , Duquet A , Moss EG , Harel-Bellan A. Lin-28 binds IGF-2 mRNA and participates in skeletal myogenesis by increasing translation efficiency. *Genes Dev*. 2007;21:1125–1138.
9. Qiu C , Ma Y , Wang J , Peng S , Huang Y. Lin28-mediated post-transcriptional regulation of Oct4 expression in human embryonic stem cells. *Nucleic Acids Res*. 2010;38:1240–1248.
10. Xu B , Huang Y. Histone H2a mRNA interacts with Lin28 and contains a Lin28-dependent posttranscriptional regulatory element. *Nucleic Acids Res*. 2009;37:4256–4263.
11. Xu B , Zhang K , Huang Y. Lin28 modulates cell growth and associates with a subset of cell cycle regulator mRNAs in mouse embryonic stem cells. *RNA*. 2009;15:357–361.
12. Ong KK , Elks CE , Li S, et al.. Genetic variation in LIN28B is associated with the timing of puberty. *Nat Genet*. 2009;41:729–733.
13. Sulem P , Gudbjartsson DF , Rafnar T, et al.. Genome-wide association study identifies sequence variants on 6q21 associated with age at menarche. *Nat Genet*. 2009;41:734–738.
14. He C , Kraft P , Chen C, et al.. Genome-wide association studies identify loci associated with age at menarche and age at natural menopause. *Nat Genet*. 2009;41:724–728.
15. Perry JR , Stolk L , Franceschini N, et al.. Meta-analysis of genome-wide association data identifies two loci influencing age at menarche. *Nat Genet*. 2009;41:648–650.
16. Elks CE , Perry JR , Sulem P, et al.. Thirty new loci for age at menarche identified by a meta-analysis of genome-wide association studies. *Nat Genet*. 2010;42:1077–1085
17. Zhu H , Shah S , Shyh-Chang N, et al.. Lin28a transgenic mice manifest size and puberty phenotypes identified in human genetic association studies. *Nat Genet*. 2010;42:626–630.
18. Balzer E , Heine C , Jiang Q , Lee VM , Moss EG. LIN28 alters cell fate succession and acts independently of the let-7 microRNA during neurogliogenesis in vitro. *Development*. 2010;137:891–900.
19. Griswold MD , Oatley JM. Concise review: defining characteristics of mammalian spermatogenic stem cells. *Stem Cells*. 2013;31:8–11.
20. De Rooij DG , Griswold MD. Questions about spermatogonia posed and answered since 2000. *J Androl*. 2012;33:1085–1095.
21. de Rooij DG , Russell LD. All you wanted to know about spermatogonia but were afraid to ask. *J Androl*. 2000;21:776–798.
22. Phillips BT , Gassei K , Orwig KE. Spermatogonial stem cell regulation and spermatogenesis. *Philos Trans R Soc Lond B Biol Sci*. 2010;365:1663–1678.

23. He Z , Kokkinaki M , Pant D , Gallicano GI , Dym M. Small RNA molecules in the regulation of spermatogenesis. *Reproduction*. 2009;137:901–911.
24. Yan N , Lu Y , Sun H, et al.. Microarray profiling of microRNAs expressed in testis tissues of developing primates. *J Assist Reprod Genet*. 2009;26:179–186.
25. Wu Q , Song R , Ortogero N, et al.. The RNase III enzyme DROSHA is essential for microRNA production and spermatogenesis. *J Biol Chem*. 2012;287:25173–25190.
26. Tong MH , Mitchell DA , McGowan SD , Evanoff R , Griswold MD. Two miRNA clusters, Mir-17-92 (Mirc1) and Mir-106b-25 (Mirc3), are involved in the regulation of spermatogonial differentiation in mice. *Biol Reprod*. 2012;86:72.
27. Zheng K , Wu X , Kaestner KH , Wang PJ. The pluripotency factor LIN28 marks undifferentiated spermatogonia in mouse. *BMC Dev Biol*. 2009;9:38.
28. Aeckerle N , Eildermann K , Drummer C, et al.. The pluripotency factor LIN28 in monkey and human testis: a marker for spermatogonial stem cells? *Mol Hum Reprod*. 2012;18:477–488.
29. West JA , Viswanathan SR , Yabuuchi A, et al.. A role for Lin28 in primordial germ-cell development and germ-cell malignancy. *Nature*. 2009;460:909–913.
30. Cao D , Allan RW , Cheng L, et al.. RNA-binding protein LIN28 is a marker for testicular germ cell tumors. *Hum Pathol*. 2011;42:710–718.
31. Gillis AJ , Stoop H , Biermann K, et al.. Expression and interdependencies of pluripotency factors LIN28, OCT3/4, NANOG and SOX2 in human testicular germ cells and tumours of the testis. *Int J Androl*. 2012;34:e160–e174.
32. Garcia-Galiano D , van Ingen Schenau D , Leon S, et al.. Kisspeptin signaling is indispensable for neurokinin B, but not glutamate, stimulation of gonadotropin secretion in mice. *Endocrinology*. 2012;153:316–328.
33. Ahmed EA , de Rooij DG. Staging of mouse seminiferous tubule cross-sections. *Methods Mol Biol*. 2009;558:263–277.
34. Garcia-Galiano D , Pineda R , Ilhan T , Castellano JM, et al.. Cellular distribution, regulated expression, and functional role of the anorexigenic peptide, NUCB2/nesfatin-1, in the testis. *Endocrinology*. 2012;153:1959–1971.
35. Barreiro ML , Gaytan F , Castellano JM, et al.. Ghrelin inhibits the proliferative activity of immature Leydig cells in vivo and regulates stem cell factor messenger ribonucleic acid expression in rat testis. *Endocrinology*. 2004;145:4825–4834.
36. Garcia-Galiano D , Navarro VM , Roa J , Ruiz-Pino F, et al.. The anorexigenic neuropeptide, nesfatin-1, is indispensable for normal puberty onset in the female rat. *J Neurosci*. 2010;30:7783–7792.
37. Roush S , Slack FJ. The let-7 family of microRNAs. *Trends Cell Biol*. 2008;18:505–516.
38. de Rooij DG. Proliferation and differentiation of spermatogonial stem cells. *Reproduction*. 2001;121:347–354.
39. Viswanathan SR , Daley GQ , Gregory RI. Selective blockade of microRNA processing by Lin28. *Science*. 2008;320:97–100.
40. McLean DJ , Friel PJ , Johnston DS , Griswold MD. Characterization of spermatogonial stem cell maturation and differentiation in neonatal mice. *Biol Reprod*. 2003;69:2085–2091.
41. Yoshida S , Sukeno M , Nakagawa T, et al.. The first round of mouse spermatogenesis is a distinctive program that lacks the self-renewing spermatogonia stage. *Development*. 2006;133:1495–1505.
42. Vergouwen RP , Huiskamp R , Bas RJ , Roepers-Gajadien HL , Davids JA , de Rooij DG. Postnatal development of testicular cell populations in mice. *J Reprod Fertil*. 1993;99:479–485.
43. Shinohara T , Orwig KE , Avarbock MR , Brinster RL. Remodeling of the postnatal mouse testis is accompanied by dramatic changes in stem cell number and niche accessibility. *Proc Natl Acad Sci U S A*. 2001;98:6186–6191.
44. Hess RA , Chen P. Computer tracking of germ cells in the cycle of the seminiferous epithelium and prediction of changes in cycle duration in animals commonly used in reproductive biology and toxicology. *J Androl*. 1992;13:185–190.
45. Carrell DT , Emery BR , Hammoud S. Altered protamine expression and diminished spermatogenesis: what is the link? *Hum Reprod Update*. 2007;13:313–327.
46. Tanaka H , Baba T. Gene expression in spermiogenesis. *Cell Mol Life Sci*. 2005;62:344–354.
47. Papaioannou MD , Nef S. microRNAs in the testis: building up male fertility. *J Androl*. 2010;31:26–33.
48. Yan W , Ma L , Burns KH , Matzuk MM. HILS1 is a spermatid-specific linker histone H1-like protein implicated in chromatin remodeling during mammalian spermiogenesis. *Proc Natl Acad Sci U S A*. 2003;100:10546–10551.
49. Tong MH , Mitchell D , Evanoff R , Griswold MD. Expression of Mirlet7 family microRNAs in response to retinoic acid-induced spermatogonial differentiation in mice. *Biol Reprod*. 2011;85:189–197.
50. Zhang FP , Poutanen M , Wilbertz J , Huhtaniemi I. Normal prenatal but arrested postnatal sexual development of luteinizing hormone receptor knockout (LuRKO) mice. *Mol Endocrinol*. 2001;15:172–183.